

# Catalytic Molecular Walkers: Aspects of Product Release

Darko Stefanovic<sup>1</sup>, Milan N. Stojanovic<sup>2</sup>, Mark J. Olah<sup>1</sup> and Oleg Semenov<sup>1</sup>

<sup>1</sup>University of New Mexico, Albuquerque, NM 87131, USA

<sup>2</sup>Columbia University, New York, NY 10032, USA

darko@cs.unm.edu

## Abstract

We study a model of multi-legged catalytic molecular walkers that abstract a class of recently developed synthetic molecular motors. We focus on their kinetics of release of catalytic product, delineating the influence of chemical kinetic parameters, geometric configuration, and loss from surface, and also contrast with bulk kinetics of product release. We show that molecular walkers can achieve a uniform rate of release over long time scales, which can be exploited in applications.

## Introduction

Nanoscale objects are subject to random Brownian motion that leads to undirected diffusive transport. Nanoscale systems that require more precise control over the transport of materials and information must expend energy in some form to bias the random molecular motion in useful directions. A *molecular motor* is a nanoscale device that is capable of transforming chemical free energy into useful work and directed motion, and can function as a cargo transport device allowing superdiffusive transport of materials. Natural molecular motors play an important role in critical biological processes in the cell and are the source of most forms of motion in living beings (Schliwa and Woehlke, 2003; Vale and Milligan, 2000; Phillips et al., 2013).

In addition to naturally occurring molecular motors, several synthetic molecular motors have been designed recently (Yin et al., 2004; Bath and Turberfield, 2007; Muscat et al., 2011; Wickham et al., 2012; Shin and Pierce, 2004; Venkataraman et al., 2007; Omabegho et al., 2009; von Delius et al., 2010; Kay et al., 2007). We have synthesized catalytic DNA-based walkers called *molecular spiders* (Pei et al., 2006). A molecular spider has a rigid body and several flexible enzymatic legs that attach to and modify substrate DNA molecules (Figure 2a). When we first reported molecular spiders, we were keen to explore their motive properties and subsequently we experimentally demonstrated their ability to follow patterned nanoscale tracks of DNA substrate molecules (Lund et al., 2010). Our mathematical modelling efforts similarly were focused on characterizing the spiders' walking gaits, such as predicting their

ability to do organized mechanical work in opposition to an external force (which we hope experimentally to validate in the near future). On the other hand, in the original study we also observed excellent chemical processivity of the spiders. In one assay, spiders and their substrates were randomly deposited in a matrix in a 1:3800 ratio, upon which the spiders cleaved nearly all the substrates (i.e., released all the available products) before dissociating from the matrix (Figure 1). We noted the nearly linear rate of substrate cleavage in this case, but this observation has not been explained or exploited.

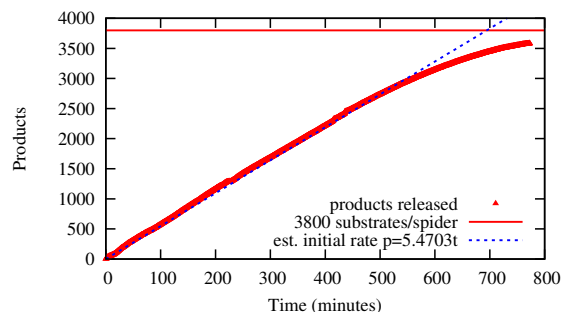


Figure 1: Data from a surface-plasmon resonance experiment. Four-legged spiders were released into a 2½D dextran matrix displaying the substrates. There were 3800 substrates to each spider, and over the course of the assay the spiders cleaved 100% of the substrate offered, exhibiting an initial linear increase in the amount of released product. (After Pei et al. (2006).)

In separate studies, we have shown that the deoxyribozyme chemistry of the spiders' legs is compatible with actuation, such as the release of small molecules (Kolpashchikov and Stojanovic, 2005; Yashin et al., 2007), as well as controllable by both oligonucleotides (Stojanovic et al., 2002) and small-molecule ligands (Stojanovic and Kolpashchikov, 2004), including via complex decision-making molecular logic (Macdonald et al., 2006). Therefore, the sustained nearly uniform rate of release from a ma-

trix, mediated by activated spiders (or other multivalent catalytic walker chemistries), may have promise in drug delivery. Indeed, achieving zero-order kinetics of drug release is a long-standing but difficult goal of pharmacokinetics (Siepmann et al., 1999; Siepmann and Peppas, 2000; Gupta and Kumar, 2000; Agrawal et al., 2006; Kim, 1995); a new study shows the use of nanoparticles to approximate it (Gu et al., 2013).

Here we numerically study the product-release properties of molecular spiders and show that:

1. walker-mediated release of product can be an effective tool for achieving a uniform rate of release over long time scales;
2. catalytic bias is essential for the operation of this mechanism;
3. catalytic bias is an effective tool for regulation of release rate;
4. multivalency is a practical mechanism for overcoming the problem of dissociation (confirming the results of Samii et al. (2010); Olah and Stefanovic (2013)).

The results provide a first guide to the vast parameter space available to the designers of potential molecular-spider-based drug delivery vehicles.

## Molecular Spiders and Their Models

We model the motion of multipedal enzymatic walkers as they move over and modify chemical sites arranged as arbitrary 2D tacks and patterns (Figure 2b). A walker has a rigid body with attachment points for  $k \geq 2$  identical, flexibly tethered legs. Each leg has a reactive site at its foot that can reversibly bind to and enzymatically modify surface-bound chemical sites from a substrate species into a product species. As a walker moves over a surface of substrate sites, the enzymatic actions of the legs leave behind a trail of modified product sites. These modified sites create an asymmetrical distribution of substrates around the walker. If the leg-product binding is weaker than the leg-substrate binding, this local substrate asymmetry can bias the motion of the walker away from previously visited areas and towards unvisited sites, causing an otherwise unbiased symmetric walker to move superdiffusively. Thus, the walkers transform the chemical free energy in the surface sites into directional motion and can do ordered work in opposition to an external load force, hence they are a new type of molecular motor, useful for directional transport in nanoscale systems.

We formulate the model as a continuous-time Markov process that describes the stochastic motion of the walker as a sequence of transitions between discrete chemical states. Each walker state is described by the chemical state of the surface sites (substrate or product) and the current set of sites where a leg is attached. The transitions from state to state

correspond to the discrete chemical actions of legs binding to sites, unbinding from sites, or enzymatically modifying attached substrate sites to products. From any particular chemical state of the walker legs, each individual chemical action is independent of the previous state of the walker and of the chemical state of the other legs. In other words, the legs are not kinetically coupled. They are, however, mechanically constrained by their connection to a common body.

We have used Monte Carlo algorithms to simulate the motion of multivalent random walkers. When the rate of substrate catalysis is much slower than the rate of product detachment, the walkers (on average) begin to move superdiffusively away from the origin. In our previous study (Olah and Stefanovic, 2013) of walkers on a track (Figure 2c), we found that the superdiffusive motion of the walker persists even under moderate opposing load forces of  $\leq 2.0$  pN, for legs with maximum extension length  $\ell = 12.5$  nm ( $2.5 \times$  the lattice pitch). Hence, the walkers are capable of transforming the chemical free energy of substrate molecules into directed transport and ordered mechanical work. We designed the model to investigate a minimal set of mechanical and kinetic features that are necessary to transform the otherwise unbiased diffusive motion of multipedal enzymatic walkers into directional, superdiffusive motion useful for nanoscale cargo transport: even though a walker's legs are identical, unoriented, uncoordinated, and unconstrained other than the passive constraint implied by their connection to a common body, nonetheless we find that these simple geometric constraints on the legs combined with the kinetic bias in the direction of unvisited substrates suffice to generate superdiffusive motion, even when that motion is opposed by an external load force.

While this model provides good physical detail, it can be computationally rather demanding, which justifies mathematical models of molecular spiders at higher levels of abstraction, for instance, simplifying the chemical kinetics and the geometry of the walker and its track. Antal and collaborators studied a single simplified spider on a one-dimensional track (Antal et al., 2007; Antal and Krapivsky, 2007), showing that a difference in residence time between substrates and products, in conjunction with the presence of multiple legs, biases the motion towards fresh substrates when the spider is on a boundary between substrates and products. We showed that this bias makes spiders move superdiffusively for long periods of time (Semenov et al., 2011a). Samii et al. investigated various gaits and numbers of legs (Samii et al., 2010, 2011), emphasizing the possibility of detachment from a 1D track. We studied the behavior of multiple spiders continuously released onto a 1D track (Semenov et al., 2011b, 2012) from a point source. Related to the present topic, Antal and Krapivsky evaluated the diffusion constant and the amplitude describing the asymptotic behavior of the number of visited sites (i.e., released products) for a single simplified spider on an infinite square

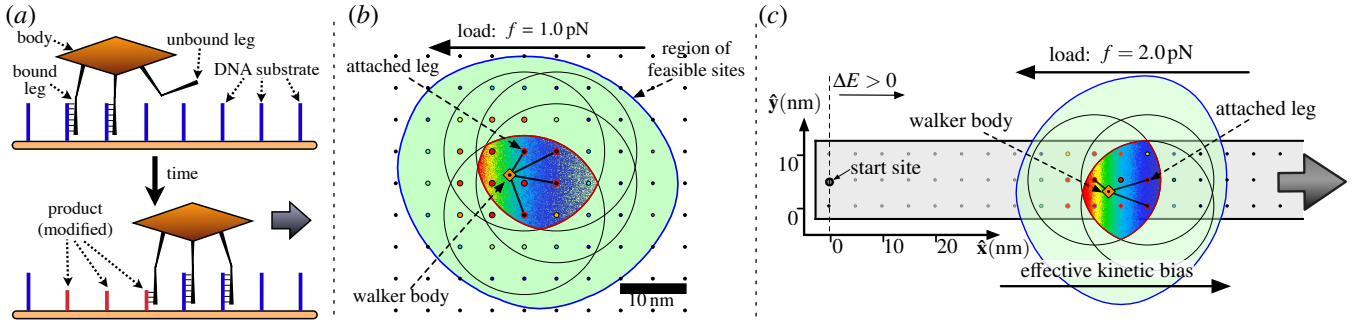


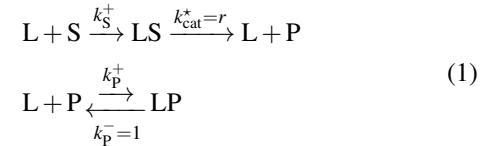
Figure 2: The general multivalent random walker model describes the motion of multipedal walkers acting as molecular motors as they move over tracks of surface-bound substrate fuel. (a) The model is inspired by a type of DNA nanowalker called a *molecular spider* that has a rigid, inert body and several enzymatic legs that can attach to and cleave complementary DNA substrates arrayed as nanoscale tracks. (b) The model describes the 2D motion of molecular-spider-like walkers. We assume the mechanical motion of the body and of its legs comes to an equilibrium in between chemical steps, allowing us to describe the attachment likelihood over the set of local feasible attachment sites. The position of the walker body is kinematically constrained by the currently attached legs to lie within a feasible region, an intersection of circles of radius  $\ell$  (red outline). Within this region, a Boltzmann distribution describes the probability of the body positions. We illustrate a leftward external load force on the body skewing the distribution to the left (warmer colors correspond to higher probability). The body is drawn at the mean of the distribution. An unattached leg seeking its next attachment point is kinematically constrained to remain within a distance  $\ell$  of some feasible body position, which results in the region of feasible sites for attachment (shaded green). The likelihood of attachment to a point is a convolution over the body position distribution; greater likelihood is indicated by larger circles and warmer colors. (c) A simulated experiment to show motor properties of the walkers on a track of substrates (Olah and Stefanovic, 2013). Under appropriate kinetic biases between product and substrate sites, the walkers move superdiffusively rightward in the transient, even when their motion is opposed by a leftward conservative load force; during the transient, the walkers do positive mechanical work against the force.

lattice (Antal and Krapivsky, 2012).

## Model Definition

The formal model we assume in this paper is a minor simplification of our general model above. In the context of a product-release application, as opposed to transport, we need not be concerned with external forces, and therefore we can set them to zero, which makes all feasible body positions equally likely; this eliminates the need for expensive equilibrium Monte Carlo computations in the inner loop of the simulation. Further, we can approximate the region of feasible sites (Figure 2(b)) as the intersection of circles of radius  $2\ell$  around all current attachment points, omitting an explicit representation of the walker body altogether; this eliminates the need for elaborate computational geometry calculations. Finally, we assume all sites within the feasible region are equally likely to be chosen as the next attachment point for the leg that is moving. Given that we wish to model multiple walkers, we assume that they interact only through the mutual exclusion of the legs.

The chemical reaction scheme is



showing an essentially irreversible binding of an enzymatic leg L to a substrate S to form a complex LS, which leads irreversibly to the cleavage of the surface-bound substrate into two product parts. The scheme only shows the part P that remains bound to the surface; the other is released into the environment, and is in fact the product part of interest in applications. The second reaction describes the fleeting, reversible, binding of a leg to the surface-bound products. The rate  $r$  encapsulates both the catalytic cleavage of the substrate and the subsequent dissociation of the leg from the products. The rate of dissociation from products is set to 1, i.e., our model is dimensionless.

We use kinetic Monte Carlo simulation (Bortz et al., 1975; Voter, 2007) to generate trajectories of the model for various parameter combinations. The implementation techniques we use are standard; of note, the results in this paper were generated with a highly customizable representation written in Haskell. Many techniques exist in the literature for speed-

ing up KMC simulations by caching the transition rates; here the set of transitions is highly dynamic and we omitted any attempts at optimization.

## Results

We have obtained simulation results for the following product release scenario. The walking surface contains 40,000 sites in a  $200 \times 200$  box in a 2D square lattice, initially consisting entirely of substrates. One hundred walkers are deposited uniformly at random onto the surface, each walker having one leg attached to a substrate and the remaining legs free. This gives a 1:400 ratio of walkers to substrates, a scaled-down version of the laboratory experiments. The walkers are followed as they move around the box until all substrates have been turned into products.

We observe the number of products on the surface, which is equal to the number of products released into the surrounding medium. We do not model the diffusion of released products into the environment. To control for the possibility of walker dissociation, we also observe the number of walkers left on the surface.

We study the effects of spider geometry by varying the number of legs from 1 to 6. In the plots that follow, only 2-, 4-, and 6-legged walkers are shown, for clarity. One-legged walkers dissociate from the surface immediately; 3- and 5-legged walkers have intermediate behaviors as expected. We also vary the leg length. We use the length  $\ell$  equal to 2.5 times the lattice pitch as our baseline, and also consider what happens if the legs are much shorter,  $\ell = 1$ , or longer,  $\ell = 5$ .

We study the effects of different chemical kinetics by varying the catalytic rate parameter  $r$ , i.e., the degree of residence-time bias between substrates and products. We also vary the binding rate parameters  $k_S^+$  and  $k_P^+$ .

### Baseline observations

Shown in Figure 3 are plots for product release using a baseline set of parameter values (Olah and Stefanovic, 2013),  $r = 0.01$ ,  $k_P^+ = 1000.0$ ,  $k_S^+ = 1000.0$ ,  $\ell = 2.5$ , and for three different leg configurations, 2-, 4-, and 6-legged. We denote the number of products released by time  $t$  as  $N(t)$ .

Consider the product release curve for the four-legged walkers (green). It rises essentially linearly for a long time before tapering off towards the ceiling of 40,000 as eventually all sites are turned into products. In this respect the model captures the empirical observations from Figure 1. Also drawn in green are two theoretical curves. The dashed line corresponds to exactly linear product release at a rate equal to the initial rate for the walker (zero-order kinetics). Note that the initial rate of product release for the walker is easily seen to be the product of the substrate catalysis-dissociation rate, which we are calling  $r$ , and the number of legs, since almost immediately upon deposition all legs are on substrates. The dotted line corresponds to an exponential decay that starts with an initial rate equal to the walker's,

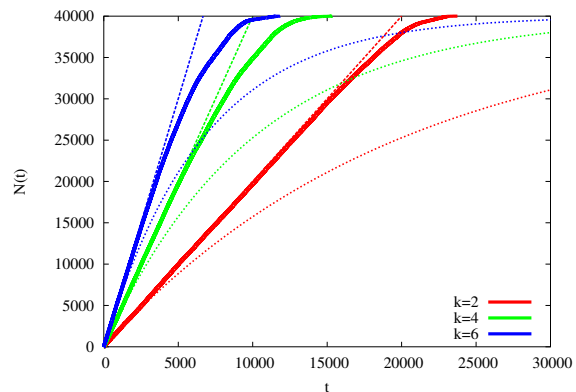


Figure 3: Number of products released as a function of time for 2-, 4-, and 6-legged walkers (solid lines), with  $r = 0.01$ ,  $k_P^+ = 1000.0$ ,  $k_S^+ = 1000.0$ , and  $\ell = 2.5$ . The observed curves are bracketted by theoretical curves for zero-order product release (dashed lines) and first-order product release (dotted lines).

and tends to the same asymptotic value (first-order kinetics). The observed curve is bracketted between the two theoretical curves, adhering more closely to zero-order kinetics.

Analogous families of curves are shown for two-legged walkers (red) and six-legged walkers (blue). The initial slope is proportional to the number of legs because each leg is an independent enzyme, and initially all legs quickly find a substrate to bind to. Interestingly, the adherence of the observed kinetics to zero-order kinetics lasts longer for  $k = 2$  walkers than for walkers with more legs.

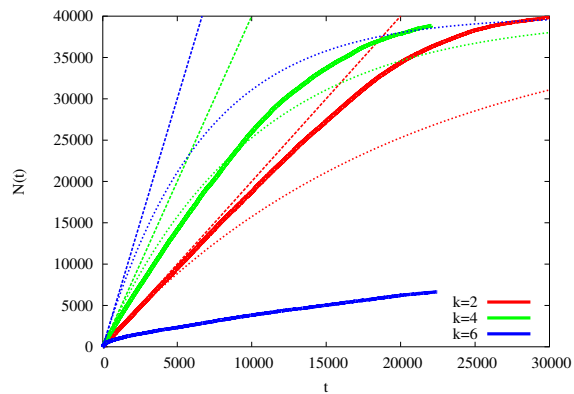
### Varying the leg length

Keeping the chemical kinetics parameters at the baseline, we vary the geometry of the walker, namely its leg length. The baseline leg length  $\ell = 2.5$  corresponds to the molecular spiders used in laboratory experiments, Figure 3. If the legs are made much shorter, as in Figure 4(a), spiders with too many legs become slower. A detached leg is too constrained by the maximum distance from the remaining legs' attachment points, and it is impeded from finding fresh substrates. Thus the product release of the two-legged walker is slower than first-order kinetics, but for the six-legged walker it is slowed down to even less than the two-legged walkers' pace.

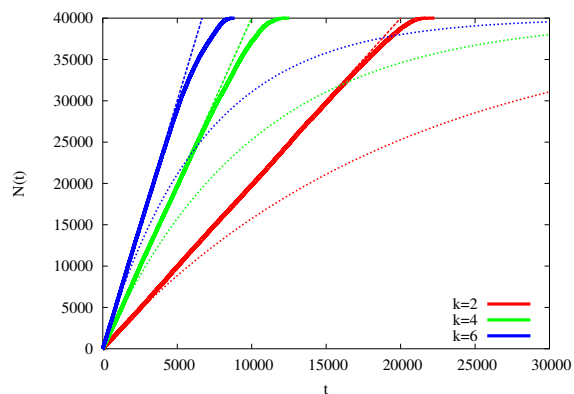
On the other hand, if the legs are made longer, as in Figure 4(b), a moving leg has a greater probability of finding a substrate when the walker is on the edge of the patch it has grazed, hence we observe better adherence to zero-order product release kinetics.

### Varying the catalysis kinetics

Here we show the effects of varying the parameter  $r$ , keeping the binding kinetics fixed at the value  $k_P^+ = 1000.0$ ,



(a) Short legs,  $\ell = 1.0$



(b) Long legs,  $\ell = 5.0$

Figure 4: Varying the leg length: number of products released as a function of time for 2-, 4-, and 6-legged walkers (solid lines). Also shown are the theoretical curves for zero-order product release (dashed lines) and first-order product release (dotted lines). The remaining parameters are  $r = 0.01$ ,  $k_p^+ = 1000.0$ , and  $k_S^+ = 1000.0$ , as in Figure 3.

$k_S^+ = 1000.0$ , which means that binding is very fast and there is no binding preference between substrates and products. Figures 5(a)–(c) display  $r = 0.001, 0.1, 1.0$ , in addition to  $r = 0.01$  from Figure 3.

The initial rate of product release varies in proportion to  $r$ , as expected because  $r$  is the hopping rate for legs on substrates. The overall time to completion grows roughly in inverse proportion to  $r$ , therefore the four plots are accordingly scaled, allowing us to observe the changes in the shapes of the curves. The adherence of the observed product release curve to the zero-order kinetics theoretical curve improves when  $r$  is decreased to 0.001 and it worsens when  $r$  is increased. When  $r$  reaches unity, and the residence-time bias is lost, product release becomes slower and less uniform even than first-order kinetics; furthermore, there is an inversion effect for the number of legs—even though initial product release rates are higher for greater  $k$ , eventually

these walkers fall behind two-legged ones.

### Varying the binding kinetics

In these simulations, we keep the catalysis fixed at the baseline value of  $r = 0.01$  but we vary the binding kinetics, i.e., the on-rates  $k_p^+$  and  $k_S^+$ .

In Figure 6, we decrease the on-rate for substrates ten-fold, so that a leg is effectively repelled from substrates. Comparing with the baseline results of Figure 3, while the initial rates (dominated by catalytic cleavage) are not affected, the product release curves diverge from zero-order kinetics much sooner, presumably because the walkers are diverted from exploration of fresh substrates and find themselves diffusing in their own local seas of product. If we also decrease the on-rate for products we recover the original behavior as in Figure 3 (we reserve for future study the effects of decreasing the two on-rates further towards the catalysis rate, outside of the regime of rates measured for deoxyribozyme walkers).

### Dissociation

Since in our model the legs are uncoordinated, it is possible for all legs of a walker to become detached. When that happens, the walker is removed from the simulation (indeed in control experiments (Pei et al., 2006) we had measured the rates at which dissociation happened with molecular spiders by physically washing away dissociated spiders). However, in the model, just as in the laboratory, dissociation is a rare event for the chosen baseline kinetics. In Figure 7 we show the number of walkers present, initially 100. Dissociation is a significant phenomenon only for two-legged walkers; for walkers with more legs, simultaneous detachment is unlikely. Thus, dissociation is not the primary cause of the drop-off in the product release rate; rather increased dissociation is a consequence of the decay into diffusion over products as each walker’s local area of products grows, or as the neighboring areas merge: legs on products detach much more frequently and thus the rate at which dissociation events occur is much greater.

### Discussion

Here we have studied molecular spiders as a mechanism to achieve controlled product release from a surface. As the results show, for suitable parameter settings, over long time periods the rate of release can be very steady, provided there is a catalytic bias ( $r < 1$ ) between the residence time on substrates vs. products. The value of the catalytic bias directly determines the rate of release, which is convenient for applications because the catalytic bias can be tuned by varying the substrate sequence. Furthermore, some design latitude exists in the number of legs per walker. Already with four legs the walkers do not suffer from premature dissociation from the surface.

It is instructive to compare the efficacy of product release achieved by a molecular spider system with the efficacy that could be achieved by an ideal enzymatic reaction taking place in a well-mixed solution. Let us consider the model of Equation 1 as if occurring in bulk solution, setting the initial number of substrate molecules equal to the initial number of sites in the spider system (40,000), and the initial number of enzyme molecules equal to the total number of our spiders' enzymatic legs (200 for two-legged spiders). We will also assume that the kinetic rates are the same for the two systems, which is a gross simplification, but a reasonable one in the absence of detailed studies of the tethered kinetics of deoxyribozymes. As shown in Figure 8(a), for  $r = 0.01$  bulk release (black curve) is nearly linear. On the other hand, in Figure 8(b) for  $r = 1$  bulk release amounts to exponential decay. Thus, as  $r$  is decreased from 1 towards 0, bulk release improves from first-order kinetics to zero-order kinetics. Spider release is also shown, and it is in both cases slower than the corresponding bulk release. After all, this should be expected from first principles. (1) In a well-mixed solution, all potential substrates are available to the enzyme. With spiders, this is not the case because substrates are a local resource; whenever the spider is diffusing in the sea of products, they are not available at all. (2) Eventually some spiders completely dissociate. These two effects make spider product release less efficient than with the hypothetical bulk solution reaction. Both these effects diminish as  $r$  is decreased from 1 towards 0. This explains why, for small values of  $r$ , product release by spiders is nearly as efficient as bulk release, which in turn is nearly linear. Thus, under suitable conditions, spiders are an effective mechanism that allows an enzyme to visit surface-immobilized substrates, yielding almost the same resultant kinetics as an ideal reaction in a perfectly mixed volume.

## Acknowledgments

This material is based upon work supported by the National Science Foundation under grants 1027877 and 1028238.

## References

- Agrawal, S. K., Sanabria-DeLong, N., Coburn, J. M., Tew, G. N., and Bhatia, S. R. (2006). Novel drug release profiles from micellar solutions of plapepla triblock copolymers. *Journal of Controlled Release*, 112:64–71.
- Antal, T. and Krapivsky, P. L. (2007). Molecular spiders with memory. *Physical Review E*, 76(2):021121.
- Antal, T. and Krapivsky, P. L. (2012). Molecular spiders on a plane. *Physical Review E*, 85:061927.
- Antal, T., Krapivsky, P. L., and Mallick, K. (2007). Molecular spiders in one dimension. *Journal of Statistical Mechanics: Theory and Experiment*, 2007(08):P08027.
- Bath, J. and Turberfield, A. J. (2007). DNA nanomachines. *Nature Nanotechnology*, 2(5):275–284.
- Bortz, A. B., Kalos, M. H., and Lebowitz, J. L. (1975). A new algorithm for Monte Carlo simulation of Ising spin systems. *Journal of Computational Physics*, 17(1):10–18.
- Gu, Z., Aimetti, A. A., Wang, Q., Dang, T. T., Zhang, Y., Veisoh, O., Cheng, H., Langer, R. S., and Anderson, D. G. (2013). Injectable nano-network for glucose-mediated insulin delivery. *ACS Nano*, 7(5):4194–4201.
- Gupta, K. C. and Kumar, M. N. V. R. (2000). Drug release behavior of beads and microgranules of chitosan. *Biomaterials*, 21:1115–1119.
- Kay, E. R., Leigh, D. A., and Zerbetto, F. (2007). Synthetic molecular motors and mechanical machines. *Angewandte Chemie International Edition*, 46(1-2):72–191.
- Kim, C. (1995). Compressed donut-shaped tablets with zero-order release kinetics. *Pharmaceutical Research*, 12(7):1045–1048.
- Kolpashchikov, D. M. and Stojanovic, M. N. (2005). Boolean control of aptamer binding states. *Journal of the American Chemical Society*, 127(32):11348–11351.
- Lund, K., Manzo, A. J., Dabby, N., Michelotti, N., Johnson-Buck, A., Nangreave, J., Taylor, S., Pei, R., Stojanovic, M. N., Walter, N. G., Winfree, E., and Yan, H. (2010). Molecular robots guided by prescriptive landscapes. *Nature*, 465:206–210.
- Macdonald, J., Li, Y., Sutovic, M., Lederman, H., Pendri, K., Lu, W., Andrews, B. L., Stefanovic, D., and Stojanovic, M. N. (2006). Medium scale integration of molecular logic gates in an automaton. *Nano Letters*, 6(11):2598–2603.
- Muscat, R. A., Bath, J., and Turberfield, A. J. (2011). A programmable molecular robot. *Nano Letters*, 11(3):982–987.
- Olah, M. J. and Stefanovic, D. (2013). Superdiffusive transport by multivalent molecular walkers moving under load. *Phys. Rev. E*, 87:062713.
- Omabegho, T., Sha, R., and Seeman, N. C. (2009). A bipedal DNA brownian motor with coordinated legs. *Science*, 324(5923):67–71.
- Pei, R., Taylor, S. K., Stefanovic, D., Rudchenko, S., Mitchell, T. E., and Stojanovic, M. N. (2006). Behavior of polycatalytic assemblies in a substrate-displaying matrix. *Journal of the American Chemical Society*, 128(12):12693–12699.
- Phillips, R., Kondev, J., Theriot, J., and Garcia, H. G. (2013). *Physical Biology of the Cell*. Garland Science, London and New York, 2nd edition.
- Samii, L., Blab, G. A., Bromley, E. H. C., Linke, H., Curmi, P. M. G., Zuckermann, M. J., and Forde, N. R. (2011). Time-dependent motor properties of multipedal molecular spiders. *Phys. Rev. E*, 84:031111.
- Samii, L., Linke, H., Zuckermann, M. J., and Forde, N. R. (2010). Biased motion and molecular motor properties of bipedal spiders. *Phys. Rev. E*, 81:021106.
- Schliwa, M. and Woehlke, G. (2003). Molecular motors. *Nature*, 422(6933):759–765.

- Semenov, O., Olah, M., and Stefanovic, D. (2012). Cooperative linear cargo transport with molecular spiders. *Natural Computing*, pages 1–18.
- Semenov, O., Olah, M. J., and Stefanovic, D. (2011a). Mechanism of diffusive transport in molecular spider models. *Physical Review E*, 83(2):021117.
- Semenov, O., Olah, M. J., and Stefanovic, D. (2011b). Multiple molecular spiders with a single localized source—the one-dimensional case. In *DNA 17: Proceedings of The Seventeenth International Meeting on DNA Computing and Molecular Programming*, volume 6397 of *Lecture Notes in Computer Science*, pages 204–216. Springer.
- Shin, J.-S. and Pierce, N. A. (2004). A synthetic DNA walker for molecular transport. *Journal of the American Chemical Society*, 126(35):10834–10835.
- Siepmann, J., Kranz, H., Bodmeier, R., and Peppas, N. A. (1999). Hpmc-matrices for controlled drug delivery: A new model combining diffusion, swelling, and dissolution mechanisms and predicting the release kinetics. *Pharmaceutical Research*, 16(11):1748–1756.
- Siepmann, J. and Peppas, N. A. (2000). Hydrophilic matrices for controlled drug delivery: An improved mathematical model to predict the resulting drug release kinetics (the “sequential layer” model). *Pharmaceutical Research*, 17(10):1290–1298.
- Stojanovic, M. N. and Kolpashchikov, D. M. (2004). Modular aptameric sensors. *Journal of the American Chemical Society*, 126(30):9266–9270.
- Stojanovic, M. N., Mitchell, T. E., and Stefanovic, D. (2002). Deoxyribozyme-based logic gates. *Journal of the American Chemical Society*, 124(14):3555–3561.
- Vale, R. D. and Milligan, R. A. (2000). The way things move: Looking under the hood of molecular motor proteins. *Science*, 288(5463):88–95.
- Venkataraman, S., Dirks, R. M., Rothmund, P. W. K., Winfree, E., and Pierce, N. A. (2007). An autonomous polymerization motor powered by DNA hybridization. *Nature Nanotechnology*, 2:490–494.
- von Delius, M., Geertsema, E. M., and Leigh, D. A. (2010). A synthetic small molecule that can walk down a track. *Nature Chemistry*, 2(2):96–101.
- Voter, A. (2007). Introduction to the kinetic Monte Carlo method. In Sickafus, K., Kotomin, E., and Uberuaga, B., editors, *Radiation Effects in Solids*. Springer.
- Wickham, S. F. J., Bath, J., Katsuda, Y., Endo, M., Hidaka, K., Sugiyama, H., and Turberfield, A. J. (2012). A DNA-based molecular motor that can navigate a network of tracks. *Nature Nanotechnology*, 7(3):169–173.
- Yashin, R., Rudchenko, S., and Stojanovic, M. N. (2007). Networking particles over distance using oligonucleotide-based devices. *Journal of the American Chemical Society*, 129(50):15581–15584.
- Yin, P., Yan, H., Daniell, X. G., Turberfield, A. J., and Reif, J. H. (2004). A unidirectional DNA walker that moves autonomously along a track. *Angewandte Chemie International Edition*, 43:4906–4911.

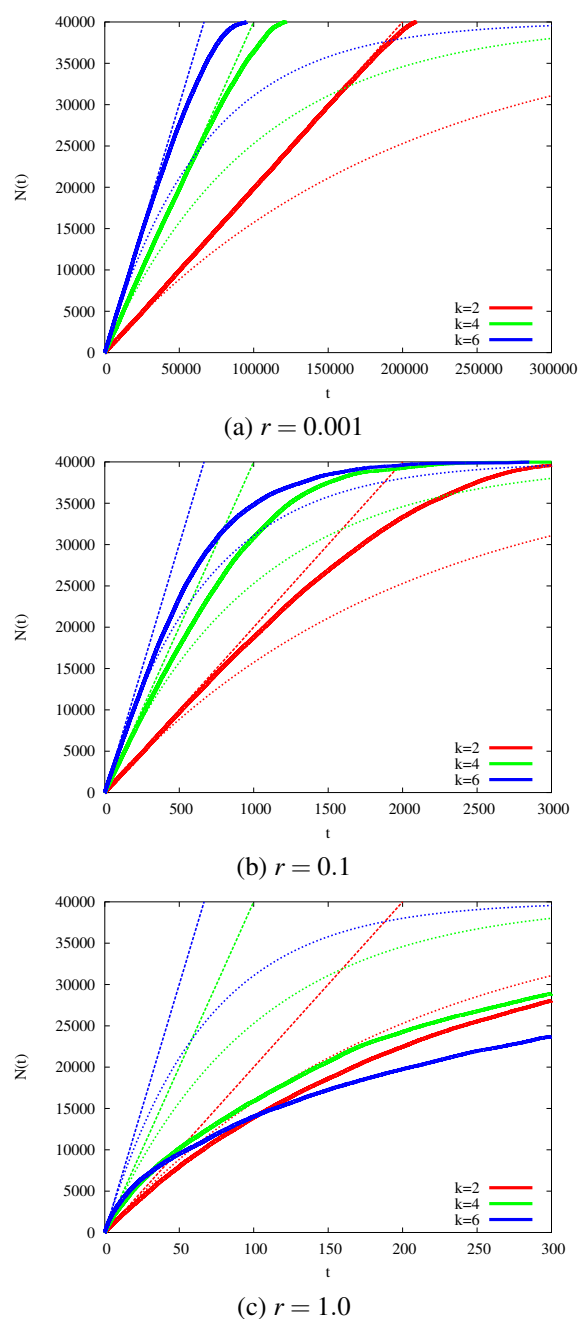


Figure 5: Varying the catalytic rate  $r$ : number of products released as a function of time for 2-, 4-, and 6-legged walkers (solid lines). Also shown are the theoretical curves for zero-order product release (dashed lines) and first-order product release (dotted lines). The remaining parameters are  $k_P^+ = 1000.0$ ,  $k_S^+ = 1000.0$ , and  $\ell = 2.5$ , as in Figure 3.

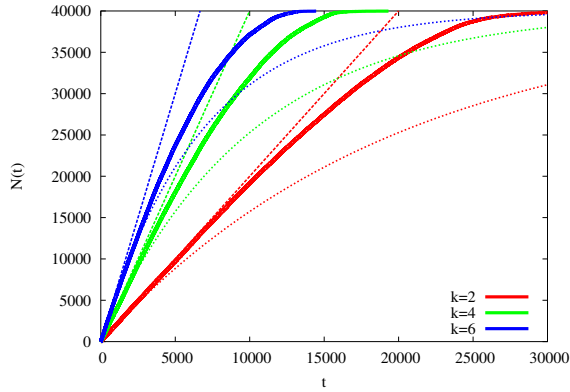
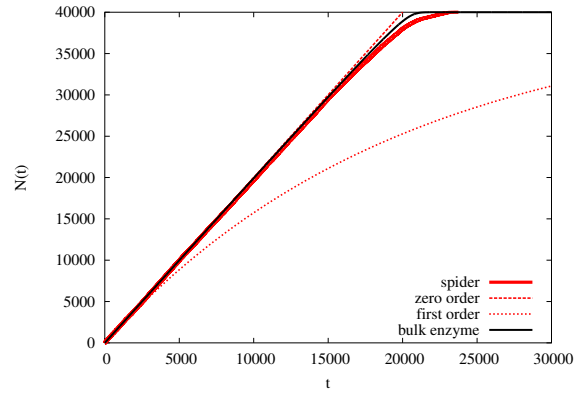
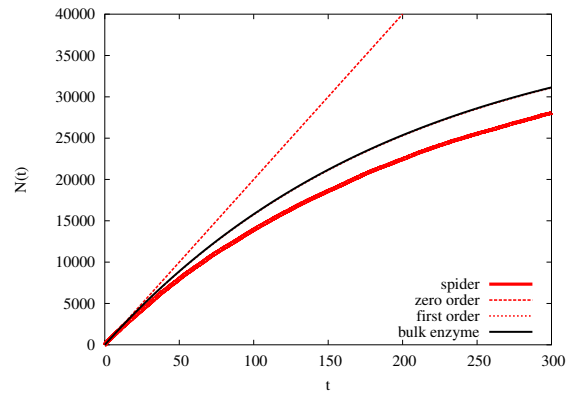


Figure 6: Varying the binding kinetics—“repellent” substrates,  $k_p^+ = 1000$ ,  $k_s^+ = 100$ : number of products released as a function of time for 2-, 4-, and 6-legged walkers (solid lines). Also shown are the theoretical curves for zero-order product release (dashed lines) and first-order product release (dotted lines). The remaining parameters are  $r = 0.01$ , and  $\ell = 2.5$ , as in Figure 3.



(a)  $r = 0.01$



(b)  $r = 1.0$

Figure 8: Comparison with bulk reaction: number of products released as a function of time, for 2-legged walkers.

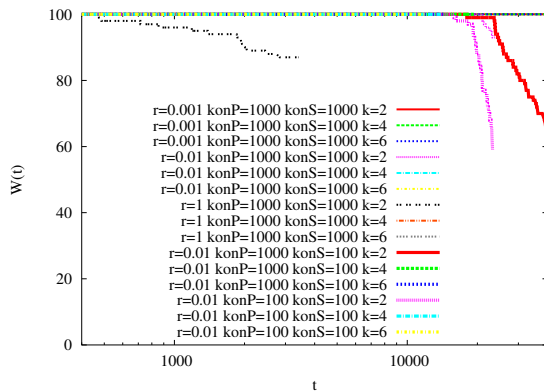


Figure 7: Number of walkers remaining as a function of time for selected configurations.